

## Cold-target recoil-ion-momentum spectroscopy study of single electron capture from He by slow Ar<sup>8+</sup> ions

M. A. Abdallah, W. Wolff,\* H. E. Wolf,\* E. Sidky, E. Y. Kamber,† M. Stöckli, C. D. Lin, and C. L. Cocke  
*J. R. Macdonald Laboratory, Physics Department, Kansas State University, Manhattan, Kansas 66506*

(Received 6 January 1998)

Cold-target recoil-ion-momentum spectroscopy (COLTRIMS) has been used to study single electron capture from He by Ar<sup>8+</sup> ions at projectile velocities between 0.2 and 1.0 a.u. Populations of  $3d$  through  $7l$  states on the final ion are resolved, and angular distributions are presented for separated major final channels. As the projectile velocity is raised, the reaction window is observed to spread. Contrary to expectations based on a Landau-Zener picture of the process, higher  $n$  and  $l$  become favored with higher  $v$ . The results are in excellent agreement with coupled-channel calculations. [S1050-2947(98)01306-7]

PACS number(s): 34.70.+e, 34.50.Fa

### I. INTRODUCTION

The capture of single electrons from neutral atomic targets by slow, highly charged ions has been heavily studied over the past decade or more, as has been summarized in several review articles [1–4]. The standard picture is that, for projectile velocities small compared to the target electron velocity, the capture proceeds at large internuclear distances at localized crossings between incident and exit channels, populating a narrow range of final states that can be predicted on the basis of several different models, including both classical barrier [5,6] and multichannel Landau-Zener models [2]. The angular distributions of the final products, which carry information about the trajectory in curve-crossing space that the reactants follow, are less accurately described by the models [1,7–12]. However, coupled-channel calculations have been able to predict both final-state distributions and, in some cases, angular distributions with remarkable accuracy in cases where the number of final channels is small enough to admit such a calculation [13,14]. As the projectile velocity is raised, it is known that eventually the curve-crossing picture is replaced by a momentum-matching one that favors capture into the most tightly bound vacant orbital on the projectile, and which allows the dominant participation of inner-shell target electrons [15]. Less experimental information is available in the intermediate region between these two extremes, partly due to the technical difficulty of doing high-resolution state-selective measurements or angular distribution measurements for higher energy projectiles. Most state-selective information that is available in this region has been obtained spectroscopically, which, although high resolution, does not allow simultaneous scattering angle measurements.

In this paper, we use cold-target recoil-ion-momentum spectroscopy (COLTRIMS) [16–18] to overcome these tech-

nical difficulties. For the case of single electron capture, the final momentum of the target ion gives uniquely the electronic energy release in the reaction, and the transverse recoil momentum gives the equivalent of the projectile scattering angle. Thus the projectile beam need not be either highly collimated or highly monoenergetic. These characteristics of COLTRIMS have been previously exploited for the study of capture by both singly [19,20] and highly charged [21,22] projectiles. In the present study, we are able to raise the projectile velocity into the region where the reaction window begins to spread substantially. We find the perhaps nonintuitive result that the first effect of this spreading is to admit the population of states with larger principal quantum numbers and higher angular momentum, rather than the population of more tightly bound final states as would be expected from a Landau-Zener argument.

The projectile Ar<sup>8+</sup> was chosen for these studies as a prototypical closed-shell ion bearing sufficient electronic charge that the splitting of the final  $l$ -states can be experimentally resolved. For this case, the subshell splitting dominates the Stark splitting of the levels of the residual ion in the field of the residual target ion. (For nearly bare projectiles, this is not the case; this case will be dealt with in a forthcoming paper.)

Single capture from He by Ar<sup>8+</sup> has been studied by several groups previously in the low velocity region. Following early total cross section measurements [23,24], Kimura and Olson [25] performed molecular orbital calculations for the  $n=4$  final states, the dominant final states, and found total cross sections in agreement with experiment. Druetta *et al.* [26] performed photon-spectroscopic measurements from which they deduced partial cross sections for  $n=4$  and  $n=5$  levels. For  $n=4$ , their results were found to be in agreement with molecular orbital calculations for  $n=4$ , as well as with the results of Kimura and Olson. These results also agreed with energy gain results of Roncin [27]. In their velocity range ( $v$  below 0.3 a.u.) little energy dependence of the cross sections was observed. Bordenave-Montesquieu *et al.* [28] and Hutton *et al.* [29] used electron spectroscopy and metastable Ar<sup>8+</sup> projectiles to study single electron capture at  $v=0.28$  a.u., and confirmed that the main populations

\*Present address: Instituto de Física, Universidade Federal do Rio de Janeiro, Caixa Postal 68.528, 21945-970 Rio de Janeiro, Brazil.

†Present address: Western Michigan University, Kalamazoo, MI 49008.

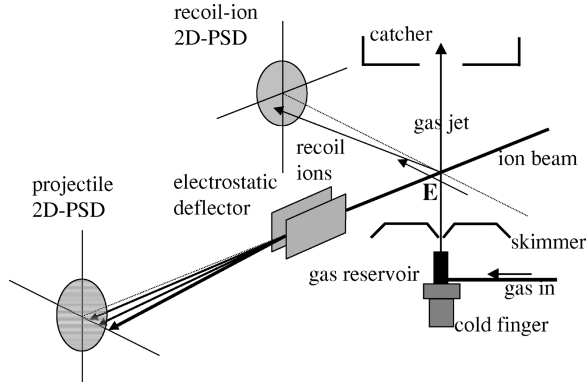


FIG. 1. Schematic of COLTRIMS apparatus used in present experiment.

were to  $n=4$ . Boudjema *et al.* [30] used a Landau-Zener model, incorporating the Olson-Salop [31] radial matrix elements, modified by the prescription of Taulbjerg to take into account nondegenerate subshells [32] to analyze both the electron and photon data, and found very good agreement with experiment. These results have been confirmed by several more recent photon-spectroscopic [33] and energy-gain measurements [33–35], all performed for projectile velocities less than 0.3 a.u.

## II. EXPERIMENT

A schematic of our COLTRIMS apparatus is shown in Fig. 1. The incident beam of 10 pA of  $\text{Ar}^{8+}$  was delivered by the KSU EBIS through a 1 mm by 1 mm aperture. It crossed a supersonically cooled He jet having a target density near  $10^{11}$  atoms/cm<sup>2</sup> and a geometrical width of 2 mm. He ions created in the interaction region were extracted by a transverse electric field of 10 to 50 V/cm and sent onto the face of a two-dimensional position-sensitive channel-plate detector (2DPSD) located 40 cm away. Meanwhile the projectile ions proceeded 3 m downstream through charge-separation plates onto the face of a second 2DPSD. In the present experiment, only the  $\text{Ar}^{7+}$  projectiles resulting from capture were allowed to hit the detector. The flight time of the He recoil was measured relative to the arrival time of the  $\text{Ar}^{7+}$  ion. The vector momentum of the He recoil was calculated from this flight time and the position at which the recoil struck the recoil detector. Using a weak focusing lens in the extractor region and an appropriate drift space, an overall momentum resolution of 0.18 a.u. (full width at half maximum) for the recoil was obtained. The data were taken in event-mode recording, whereby the positions from both detectors and the relative flight time were recorded for each event. The data cover simultaneously the final channels for single capture and transfer ionization, corresponding to the coincident detection of  $\text{He}^+$  and  $\text{He}^{2+}$  with  $\text{Ar}^{7+}$ , respectively. In this paper we analyze only the former channel.

The  $Q$  value for the reaction is related to the  $z$  momentum,  $p_z$ , of the recoil ion by [36]

$$Q = -v p_z - v^2/2, \quad (1)$$

where  $v$  is the projectile velocity (atomic units are used throughout) and the  $z$  axis lies along the beam. Here  $Q$  is the

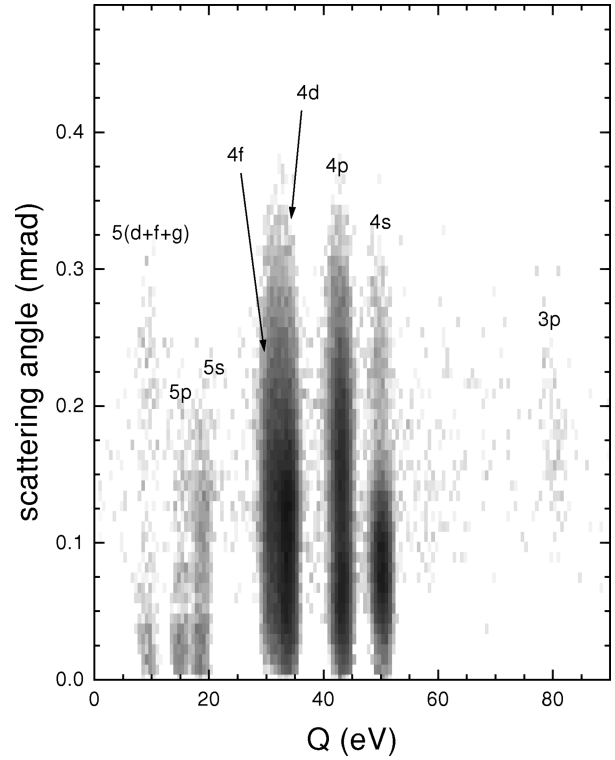


FIG. 2. Density plot of scattering angle vs  $Q$  for a projectile velocity of 0.5 a.u. The vertical axis was obtained from the recoil  $p_\perp$  using Eq. (2), while the horizontal axis was obtained from the recoil  $p_z$  using Eq. (1).

electronic energy released in the capture process, the difference between the binding energy of the final state of the  $\text{Ar}^{7+}$  ( $n, l$ ) ion and the ionization potential of the He target (24.59 eV). Thus the  $p_z$  spectrum gives directly the distribution of final state populations. The transverse recoil momentum,  $p_\perp = \sqrt{(p_x^2 + p_y^2)}$ , carries information equivalent to that of the angular scattering of the projectile, since the transverse momentum received by the recoil is exactly opposite to that received by the projectile for capture.

## III. RESULTS AND DISCUSSION

### A. General characteristics of data

Figure 2 shows a density plot of the recoil momentum spectrum for  $v = 0.5$  a.u. The horizontal axis is the  $Q$  value, obtained from  $p_z$  using Eq. (1). The vertical axis is  $p_\perp$ , presented as a projectile scattering angle ( $\theta$ ) using the equation

$$p_\perp = \theta p_0 \quad (2)$$

where  $p_0$  is the projectile beam momentum. The  $Q$ -value resolution in this spectrum is 2.4 eV, or 0.3 eV/charge. This represents 1 part in  $10^5$  of the beam energy, illustrating the advantage of the recoil method over the projectile energy-analysis method. The efficiency of the COLTRIMS system is such that the time required to accumulate a spectrum such as shown in Fig. 2 is about 2 h.

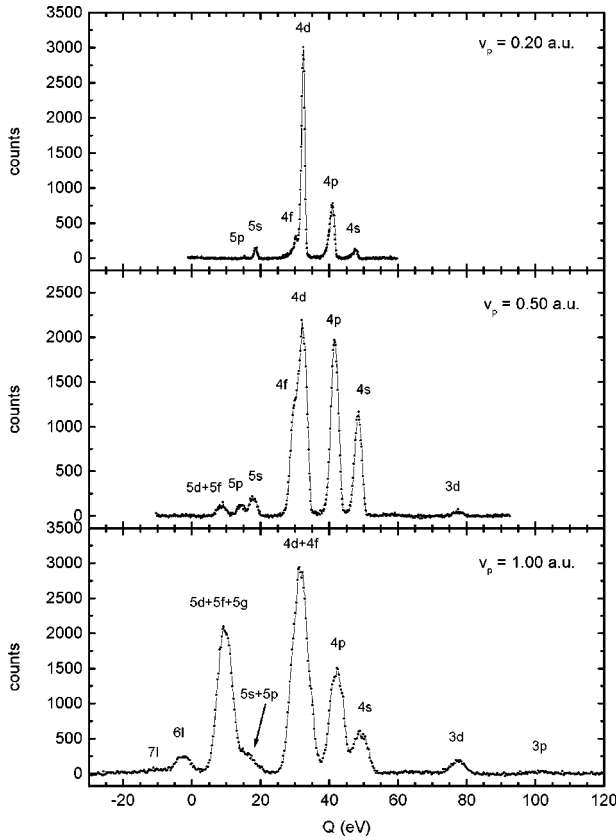


FIG. 3.  $Q$ -value spectra for three beam velocities, obtained from projecting spectra such as Fig. 2 onto the horizontal axis.

### B. Energy gain spectra

Figure 3 shows  $Q$ -value spectra obtained by projecting two-dimensional spectra such as Fig. 2 onto the horizontal axis, for three representative velocities. The population distribution for  $v=0.2$  a.u. is very close to that found by previous low-velocity experiments, with domination by the  $4d$  state and smaller contributions by  $4f$ ,  $4p$ ,  $4s$ , and  $5s$ . This final state distribution is not very velocity dependent until the velocity is raised to about 0.5 a.u. The most important initial result from raising the velocity is seen to be a spreading of the reaction window, as is seen from the center panel of Fig. 3, where the population of both the  $4f$  and  $4s$  states is seen to have become nearly equal to that of the  $4d$  and  $4p$  states. As the velocity is raised above 0.8 a.u., a rather dramatic change in the final-state population occurs that cannot simply be described as a broadening of the reaction window. A rather sudden onset of a strong population of the  $5d$ - $5g$  occurs in this region, and by the time  $v=1.0$  a.u. this group has a population comparable to that of the  $4d$ - $4f$  dominant group.

A physical explanation for the increasing importance of high angular momentum states may be that, as  $v$  increases, the electrons extracted from the target have larger angular momentum in the rest frame of the projectile and can thus populate a full distribution of the magnetic substates associated with even the higher  $l$  states. For example, the classical barrier radius for the transfer of one electron in the present case is 7 a.u., and for  $v=1$  a.u. the product of  $v$  and  $b$  is 7, which is quite large enough to account for the strong popu-

lation of states with large angular momentum projections onto an axis perpendicular to the collision plane. In the strict Landau-Zener picture of the collision, only  $\sigma$  states are involved; rotational coupling is ignored. For  $v$  at or below about 0.1 a.u., this has proved to be a reasonable assumption, and it is well established that the population of a particular state has much more to do with the location of that state within the reaction window than with its particular quantum numbers. Apart from the Taulbjerg factor [32], which describes how the coupling strength is distributed among different  $l$  for a given  $n$ , angular momentum selection rules play little role. This is no longer true for  $v$  near 1 a.u., however. Rotational coupling cannot be ignored in this region, and the full manifold of magnetic states for a given  $l$ , even for high  $l$ , comes into play.

In order to subject this speculative explanation to a quantitative test, we have performed coupled channel calculations for this system for velocities of 0.2, 0.5, and 1.0 a.u. The calculation used the procedure described by Fritsch and Lin [14] and included 41 states. All states up to  $n=5$  were implemented in the  $\text{Ar}^{8+}$  projectile center, and states up to  $n=3$  were included on the  $\text{He}^+$  target center. The close coupling calculation views the He target as a one electron atom, where the electron moves in a spherically symmetric potential, including Coulomb and screening interactions, from the  $\text{He}^+$  core:

$$V_{\text{He}}(r) = \frac{-1 - (1 + 0.65354r)e^{-2.69697r}}{r}. \quad (3)$$

Similarly the  $\text{Ar}^{8+}$  ion is treated as a frozen core from which the electron sees the potential:

$$V_{\text{Ar}}(r) = \frac{-8 - (10 + 5.5r)e^{-5.5r}}{r}. \quad (4)$$

Since the semiclassical approximation, where the internuclear motion is treated classically, is adopted here, all state amplitudes are computed as a function of impact parameter. The resulting calculated population distributions are compared with the present results in Fig. 4. It is seen that both the initial effect of reaction window spreading and the rather sudden onset of strong population of the  $5d$ - $5g$  for  $v=1$  a.u. is reproduced by the calculation. It is interesting to note that the calculation shows that most of this population increase is due to the  $5g$  state.

We note that a Landau-Zener argument could easily lead one to expect erroneously that, as  $v$  is raised, states with lower  $n$  (and  $l$ ) will become favored, since these states are those that have crossings at smaller internuclear distances, and thus have larger coupling matrix elements, and should therefore have optimal nondiabatic behavior at higher velocities than should the states that cross farther out. This behavior is seen in the predicted multichannel Landau-Zener populations also shown in Fig. 4. However, a comparison of this prediction with the data in that figure shows that the increasingly important role of rotational coupling appears to dominate any shift in the reaction window caused by the shift of

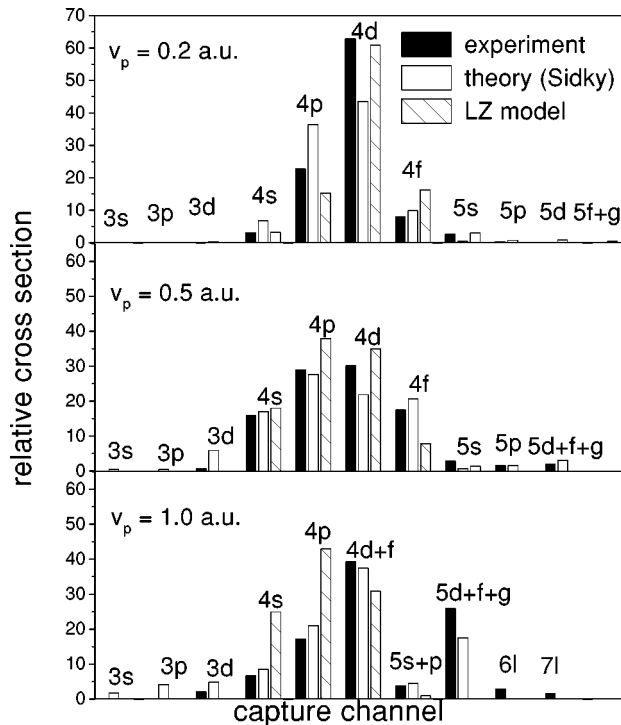


FIG. 4. Comparison of experimental and theoretical relative cross sections to various final states at three incident velocities. The cross sections are normalized to a total of 100 at each projectile velocity.

optimum nondiabaticity. The experimental result is that the centroid of the effective reaction window moves to higher  $n$  (and  $l$ ) rather than to lower  $n$ . The average  $Q$  value for the capture decreases instead of increasing. A similar qualitative effect was seen by Wu *et al.* [37] for  $O^{7+,8+}$  and  $N^{7+}$  on He in average  $Q$ -value measurements.

### C. Angular distributions

In Fig. 5 we present angular distributions for the  $4s$ ,  $4p$ , and  $4f$ - $4d$  channels for  $v=0.5$  a.u. The ‘‘half-Coulomb’’ angle ( $\theta_c$ ) for each case ( $\theta_c=Q/2E$ , where  $E$  is the beam energy [8]) is indicated by an arrow in each figure. This angle is that to which the projectile would be scattered for an impact parameter equal to the crossing radius if Coulomb potential curves are employed. It is common in the literature to discuss angular scattering for low-energy scattering by highly charged ions in terms of semiclassical trajectories along such Coulomb potential curves. Andersson and Bárány [9–11] combined such a model with a multichannel Landau-Zener model for the quantitative analysis of several collision systems [9–12]. A common result of such an approach is that the angular distributions have a minimum at the position of the half-Coulomb angle, separating regions of capture ‘‘on the way in’’ at smaller angles from capture ‘‘on the way out’’ at larger angles. This behavior has never really been seen in experiment. In order to see if some of the structure in Fig. 5 can be attributed to such features, we carried out calculations using the program of Andersson and Bárány [11] to evaluate angular distributions from this model. We compare the results to the present data in Fig. 5. In order to take approximate account of the experimental angular resolution,

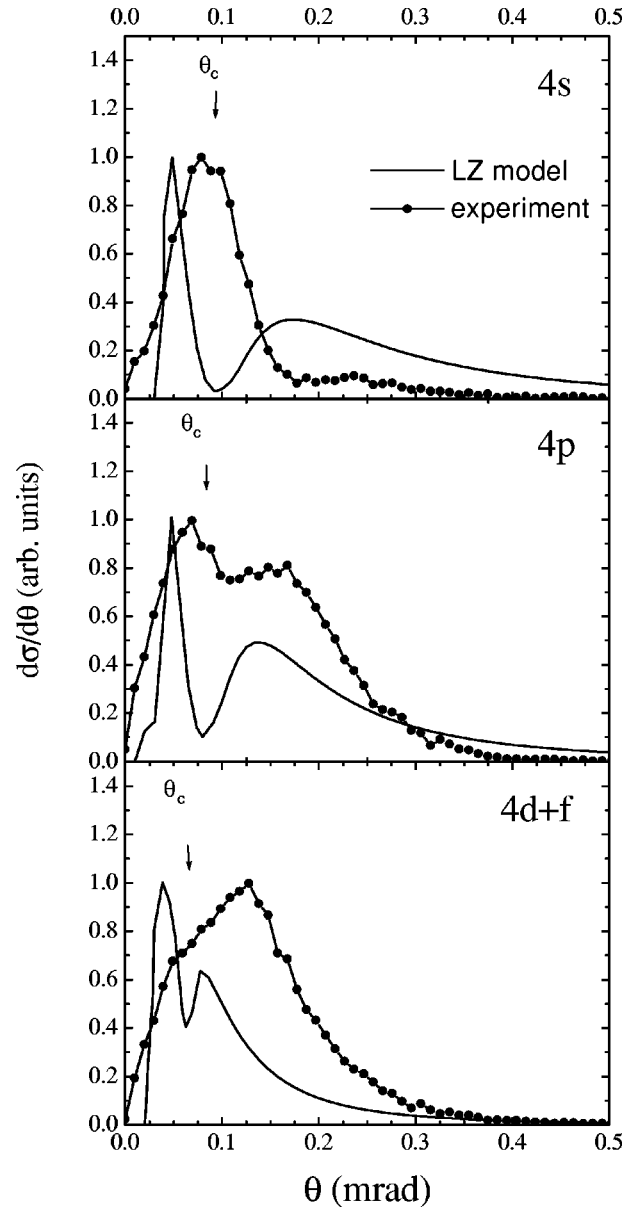


FIG. 5. Experimental angular distributions (closed circles) for the three major channels for single capture from He by 6.24 keV/u  $Ar^{8+}$  ( $v=0.5$  a.u.). The solid lines without data points are a semi-classical multichannel Landau-Zener calculation carried out using the methods of Andersson and Bárány [10,11].

we have folded the model results in Fig. 5 into a resolution function of width 0.01 mrad. The model results have been normalized to approximately match the experimental peak heights in the figure. The model assumes localized crossings for all transitions, and this assumption gives rise to step-function-like angular distributions; this behavior is of course not expected in the real data, and is not seen. There is some similarity between the data and the model result, but it is clear that this model is not adequate to describe any of the details of the present data.

Angular distributions were also calculated from the coupled-channel transition amplitudes. The standard Eikonal transformation was used to convert the amplitude dependence from impact parameter to scattering angle [38]. The-

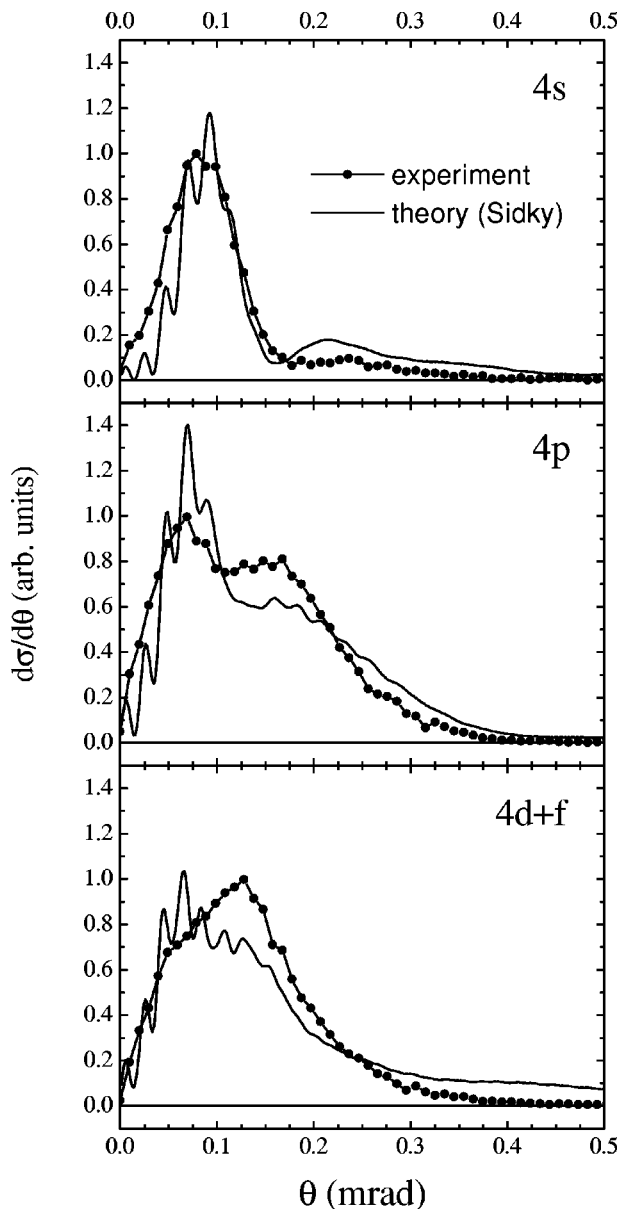


FIG. 6. Similar to Fig. 5, but showing a comparison between experiment and the coupled-channel calculation.

results are shown in Fig. 6. The agreement is seen to be very good, showing that the theoretical coupled-channel description of this collision process by this approach is nearly complete. This is a considerable feat when it is realized that 41 states must be included in the calculation. The high frequency oscillations seen in the calculation, of period near 0.02 mrad, are not seen in the experiment. This seems to be a real discrepancy between experiment and theory, since the experimental resolution of 0.01 mrad should have been adequate to resolve this structure in the present experiment, were it present in nature. However, we do not have a direct way to establish the experimental resolution from any observed sharp features in any of the transverse momentum spectra.

In spite of its failure to predict the advent of strong population of high- $l$  (and  $n$ ) states at the highest velocity, the Landau-Zener model does rather well at predicting the population distributions for the two lower velocities. It is there-

fore somewhat surprising that it fares so poorly in predicting the angular distributions. We suspect that this failure lies primarily in its incorrect prediction of the impact-parameter dependence of the reaction. The Landau-Zener (LZ) model assumes that each transition is local, taking place at the relevant crossing radius. In fact, an examination of the impact-parameter dependences from the coupled-channel calculations shows that the transitions are not nearly as localized as would be expected from the LZ calculation, and place much more weight on impact parameters inside the crossing radii than the LZ model would predict. Finally, we note that the use of the universal Olson and Salop matrix coupling element is very difficult to defend at velocities near 1 a.u., since no account of electron translational factors is taken into account in this formulation. We conclude that, while the localized-crossing picture is useful for qualitative arguments, it is probably inappropriate to press it too hard in making detailed predictions.

#### IV. SUMMARY AND CONCLUSIONS

We have presented data for single capture from He by  $\text{Ar}^{8+}$  over a velocity range extending from the “low-velocity” range ( $v=0.2$  a.u.) to the “intermediate-velocity” range ( $v\sim 1$  a.u.). The data have been obtained using COLTRIMS, which has allowed us to emerge from the low-velocity regime and to obtain high quality angular and  $Q$ -value information simultaneously over a wide velocity range. A  $Q$ -value resolution between 1.0 and 5 eV was obtained, simultaneous with a transverse momentum transfer, or projectile scattering angle, resolution of 0.005 to 0.05 mrad. The final state distributions are found to be in agreement with previous results for low  $v$ . As  $v$  is raised, two major effects are observed. First, the reaction window spreads. Second, the population of high- $l$  (and high  $n$ ) states is seen to increase rapidly. This effect is opposite to what one would expect from a Landau-Zener model.

Coupled-channel calculations using an atomic basis were performed for this system. The agreement with the data is excellent in the prediction of the final state populations, in particular the increasing importance of high  $l$  at the larger  $v$ . We attribute this to the increasing importance of rotational coupling for higher  $v$ . While a Landau-Zener treatment of the angular distributions appears inadequate, the coupled-channel calculations also describe rather well the angular distributions. It appears that the coupled-channel theoretical treatment of this process is under good control in nearly all aspects, even with such a larger number of active channels involved. An examination of the impact-parameter dependences from the calculation shows little evidence that a localized-crossing picture of the capture resembles quantitative reality.

#### ACKNOWLEDGMENTS

This work was supported by the Division of Chemical Sciences, Basic Energy Sciences, Office of Energy Research, U.S. Department of Energy. We thank A. Bárány for sending us the computer program for evaluating the Landau-Zener differential cross sections.

- [1] M. Barat and P. Roncin, *J. Phys. B* **25**, 2205 (1992).
- [2] E. K. Janev and H. Winter, *Phys. Rep.* **117**, 265 (1985).
- [3] E. K. Janev and L. P. Presnyakov, *Phys. Rep.* **70**, 1 (1981).
- [4] C. L. Cocke, in *Review of Fundamental Processes and Applications of Atoms and Ions*, edited by C. D. Lin (World Scientific, Singapore, 1993), p. 111.
- [5] H. Ryufuku, K. Sasaki, and T. Watanabe, *Phys. Rev. A* **21**, 745 (1980).
- [6] A. Niehaus, *J. Phys. B* **19**, 2925 (1986).
- [7] P. Roncin *et al.*, *J. Phys. B* **22**, 509 (1989).
- [8] L. Tunnell *et al.*, *Phys. Rev. A* **35**, 3299 (1987).
- [9] L. Andersson, H. Danared, and A. Bárány, *Nucl. Instrum. Methods Phys. Res. B* **23**, 54 (1987).
- [10] L. Andersson *et al.*, *Phys. Rev. A* **43**, 4075 (1991).
- [11] L. Andersson, Res. Inst. of Physics, Stockholm, Internal Report, No. RIPS 86:2, 1986 (unpublished).
- [12] C. Biedermann *et al.*, *Phys. Rev. A* **42**, 6905 (1990).
- [13] W. Fritsch, in *Review of Fundamental Processes and Applications of Atoms and Ions*, edited by C. D. Lin (World Scientific, Singapore, 1993), p. 239.
- [14] W. Fritsch and C. D. Lin, *Phys. Rev. A* **54**, 4931 (1996).
- [15] M. R. C. McDowell and J. P. Coleman, *Introduction to the Theory of Ion-Atom Collisions* (North-Holland, Amsterdam, 1970), p. 373.
- [16] J. Ullrich, R. Moshhammer, R. Doerner, O. Jagutzki, V. Mergel, H. Schmidt-Böcking, and L. Spielberger, *J. Phys. B* **30**, 2917 (1997).
- [17] J. Ullrich *et al.*, *Comments At. Mol. Phys.* **30**, 285 (1994).
- [18] R. Doerner *et al.*, *Nucl. Instrum. Methods Phys. Res. B* **124**, 225 (1997).
- [19] V. Mergel *et al.*, *Phys. Rev. Lett.* **79**, 387 (1997).
- [20] V. Mergel *et al.*, *Phys. Rev. Lett.* **74**, 2200 (1995).
- [21] A. Cassimi *et al.*, *Phys. Rev. Lett.* **76**, 3679 (1996).
- [22] X. Flechard *et al.*, *J. Phys. B* **30**, 3697 (1997).
- [23] E. Salzborn and A. Mueller, in *Proceedings of ICPEAC XI*, edited by N. Oda and K. Takayanagi (North-Holland, Amsterdam, 1980), p. 407.
- [24] E. Justiniano *et al.*, *Phys. Rev. A* **29**, 1088 (1984).
- [25] M. Kimura and R. E. Olson, *Phys. Rev. A* **31**, 489 (1985).
- [26] M. Druetta, S. Martin, T. Bouchama, C. Harel, and H. Jouin, *Phys. Rev. A* **36**, 3071 (1987).
- [27] P. Roncin, thèse de 3<sup>me</sup> cycle, Université de Paris, 1985 (unpublished).
- [28] A. Bordenave-Montesquieu, P. Benoit-Cattin, M. Boudjema, A. Gleizes, and S. Dousson, *Nucl. Instrum. Methods Phys. Res. B* **23**, 94 (1987).
- [29] R. Hutton, M. H. Prior, S. Chantrenne, M. H. Chen, and D. Schneider, *Phys. Rev. A* **39**, 4902 (1989).
- [30] M. Boudjema, P. Benoit-Cattin, A. B. Bordenave-Montesquieu, and A. Gleizes, *J. Phys. B* **21**, 1603 (1988).
- [31] R. E. Olson and A. Salop, *Phys. Rev. A* **14**, 579 (1976).
- [32] K. Taulbjerg, *J. Phys. B* **19**, L367 (1986).
- [33] S. Bliman *et al.*, *Phys. Rev. A* **46**, 1321 (1992).
- [34] A. Gosselin *et al.*, *J. Phys. B* **28**, 445 (1995).
- [35] H. Lebius and B. A. Huber, *Z. Phys. D (supplement)* **21**, S271 (1991).
- [36] R. Ali, V. Frohne, C. L. Cocke, M. Stöckli, S. Cheng, and M. L. A. Raphaelian, *Phys. Rev. Lett.* **69**, 2491 (1992).
- [37] W. Wu, J. P. Giese, Z. Chen, R. Ali, C. L. Cocke, R. Richard, and M. Stöckli, *Phys. Rev. A* **50**, 502 (1994).
- [38] B. H. Bransden and M. R. C. McDowell, *Charge Exchange and the Theory of Ion-Atom Collisions* (Clarendon, Oxford, 1992), p. 83.